Coalescence of stretching vortices

P. A. Jacobs and D. I. Pullin
Department of Mechanical Engineering, University of Queensland, St. Lucia, Queensland, 4067, Australia

(Received 13 August 1984; accepted 29 November 1984)

The contour dynamics numerical technique is used to study the coalescence of two equal uniform vortices in the presence of an externally applied stretching strain field. Plane three-dimensional stretching is found to substantially inhibit vortex coalescence when the plane of the vortex axes is initially perpendicular to the plane of the straining motion. This behavior is interpreted qualitatively in terms of a purely two-dimensional flow fully equivalent to the stretching configuration.

I. INTRODUCTION

Vortex-interaction models[1] in inviscid incompressible fluid mechanics have received much recent attention. Of the many codes currently available the so-called "contour dynamics" model of Zabusky, Hughes and Roberts[2,3] has proved particularly useful in the study of plane vortical flows at high Reynolds numbers. Here, for an initially piecewise constant initial vorticity field, use of the Helmholtz theorem allows reduction of the flow dynamics to an initial value or free-boundary-value problem defining the evolution of the vorticity boundaries, which may be solved numerically. In addition to Refs. 2 and 3, applications to date include the unsteady behavior of infinite vortex layers[4] and a steady flow model[5] of the finite area Von Karman vortex street.

It is well known that for many turbulent flows the essentially three-dimensional mechanics of amplification and reorientation or "tilting" of the vorticity vector by the local strain field are of critical importance for the flow dynamics. Recent turbulence models which incorporate the vortex stretching mechanism are those for lambda-vortex structure in a turbulent boundary layer (Perry and Chong[6]), the fine-scale structure of high Reynolds-number turbulence (Lundgren[7]) and the behavior of secondary, streamwise vortices in a mixing layer (Corcos and Sherman[8] and Lin and Corcos[9]). A common feature of these models is the proposed intermittent merging or coalescence of vortices in the presence of a stretching strain field provided by the average induced motion of all surrounding vortices. Lundgren assumes a pure axially symmetric stretching strain field, while Perry and Chong consider a more general field which includes a two-dimensional plane-strain component. Lin and Corcos describe numerical computations at moderate Reynolds number which show the nonlinear instability of a strained Burgers'[10] vortex sheet. Following roll-up of the shear layer into a row of finite separate vortices, they find vortex coalescence for weak stretching strain. For a larger value of the strain rate no tendency toward merging was observed over the calculated time period.

In the present paper we present computations which show qualitatively the influence of plane three-dimensional stretching strain [defined following Eq. (2)] on the inviscid merging process of two equal uniform vortices. We shall use the words "merging" and "coalescence" to synonymously describe a process distinct from that of "pairing." This last term simply denotes the tendency of a vortex pair to rotate about each other without necessary mutual contact. By contrast, in a real viscous fluid, vortex coalescence is characterized by strong diffusive exchange of vorticity between interacting partners (see, for example, the calculations of Refs. 8 and 9). For an inviscid uniform vortex model, which we suppose is appropriate at sufficiently high Reynolds numbers over some time interval, this diffusion-based definition clearly fails. Vortex coalescence then becomes a somewhat ambiguous term requiring a relative interpretation. This may be seen by noting that separate vortices in an inviscid fluid cannot actually come into mutual contact, although their boundaries might come arbitrarily close. Actual contact would imply that in a fluid with continuous velocity, initially separate fluid particles would meet at a point in a finite time, which is impossible. Thus, we shall presently view coalescence somewhat loosely as the mutual "embrace" or "folding together" of interacting finite area regions of uniform vorticity, whose boundaries have approached arbitrarily close to each other. This interpretation is consistent with the sense implied by, for example, Zabusky *et al.*[2] and Overman and Zabusky.[3]

In the following it is shown in Sec. II that the contour dynamics (CD) technique may be utilized for the study of a cylindrically symmetric vortex motion in the presence of a uniform, time-dependent stretching strain field. The initial value problem may be expressed either in terms of a timewise exponentially varying vorticity field or, using a similarity transformation,[7] as a completely equivalent constant vorticity two-dimensional vortex flow. The numerical solution method is described in Sec. III, while in Sec. IV the model is first tested against recently discovered solutions for isolated elliptical vortices and is then further applied to the stretched vortex merging configuration.

II. UNIFORM VORTICITY IN A THREE-DIMENSIONAL STRAIN FIELD

The model describes the interaction of a vorticity field and an imposed uniform three-dimensional, unsteady strain field. The initial vorticity field in (x, y, z) coordinates is given by

$$\omega = \omega_z(x, y, t = 0)\mathbf{k}, \tag{1}$$

and the imposed irrotational strain field by

 0031-9171/85/061619-07$01.90

$$\mathbf{u}_s = -\beta(t)x\mathbf{i} + [\beta(t) - \gamma(t)]\, y\mathbf{j} + \gamma(t)z\mathbf{k}, \tag{2}$$

where $\gamma(t)$ and $\beta(t)$ are arbitrary strain rates, and (i,j,k) are coordinate unit vectors along the principal strain axes. Positive $\gamma(t)$ will stretch the vorticity field in the z direction, while negative $\gamma(t)$ will give vortex compression. We shall refer to the following special cases of interest:

(i) plane two-dimensional strain $\gamma(t) = 0$,

(ii) plane three-dimensional stretching strain $\beta(t) = 0, \gamma(t) > 0$,

(iii) pure axially symmetric stretching strain $\beta(t) = \frac{1}{2}\gamma(t)$.

The full velocity field is given by

$$\mathbf{u} = u_x\mathbf{i} + u_y\,\mathbf{j} + u_z\mathbf{k}, \tag{3}$$

where

$$u_x = -\beta(t)x + V_x(x, y, t), \tag{4a}$$

$$u_y = [\beta(t) - \gamma(t)]y + V_y(x, y, t), \tag{4b}$$

$$u_z = \gamma(t)z. \tag{4c}$$

Using $\nabla \cdot \mathbf{u} = 0$ for an incompressible fluid and $\mathbf{w} = \nabla \times \mathbf{u}$, it follows that

$$\frac{\partial V_x}{\partial x} + \frac{\partial V_y}{\partial y} = 0, \tag{5a}$$

$$\omega_z = \frac{\partial V_y}{\partial x} - \frac{\partial V_x}{\partial y}. \tag{5b}$$

Hence, V_x and V_y may be derived kinematically from a cylindrically symmetric vorticity field.

The vorticity must satisfy the transport equation

$$\frac{D\boldsymbol{\omega}}{Dt} = (\boldsymbol{\omega} \cdot \nabla)\mathbf{u} + \nu\nabla^2\boldsymbol{\omega}, \tag{6}$$

where $D\omega/Dt$ is the Lagrangian derivative. On the grounds that the behavior of an inviscid model shall be relevant for a finite time, to rotational flow at high Reynolds number, we will now consider a fluid with $\nu = 0$. Substituting (1) and (4) into (6) gives

$$\frac{D\omega_z}{Dt} = \gamma(t)\omega_z. \tag{7}$$

The solution to (7) along particle paths $x(t)$, $y(t)$ is

$$\omega_z[x(t), y(t), t] = \omega_z[x(0), y(0), 0]\exp[\Omega(t)], \tag{8a}$$

$$\Omega(t) = \int_0^t \gamma(\tau)d\tau, \tag{8b}$$

where $\omega_z[x(0), y(0), 0]$ is the initial vorticity. Equations (8a) and (8b) represent the intensification of particle vorticity (for $\gamma > 0$) by the z component of the applied strain field (2).

We now simplify the model by restricting attention to M simply connected interior regions R_K, $K = 1 \cdots M$, with corresponding boundaries ∂R_K each containing an initially uniform vorticity distribution given by

$$\omega_z(x, y, 0) = \omega_0 = \text{const}, \quad (x, y) \in R_K, \quad K = 1 \cdots M,$$
$$\omega_z(x, y, 0) = 0, \quad (x, y) \notin R_K. \tag{9}$$

From (8) it follows that ω_z remains uniform in R_K for $t > 0$. Further from (5) and (9) it follows that (V_x, V_y) can be derived from a cylindrically symmetric velocity potential $\phi(x, y, t)$, $(x, y) \notin R_K$. In the absence of solid boundaries, we may then use the complex variable form of the Biot–Savart law[4] to express $V_x - iV_y$ in terms of area integrals over the R_K. Using the complex Green's theorem[4] to convert area to line integrals, and identifying $[u_x(x, y) - iu_y(x, y)]$ from (4) with particle velocities on ∂R_K then leads to a contour-dynamics formulation[2–4] for $\partial R_K(t)$, $K = 1 \cdots M$,

$$\frac{\partial x_K}{\partial t} - i\frac{\partial y_K}{\partial t} = -\beta(t)x_K + i[\gamma(t) - \beta(t)]y_K + \frac{\omega_0 \exp[\Omega(t)]}{2\pi i}\sum_{J=1}^{M}\oint_{\partial R_J}\frac{y_K - y_J'}{\sigma_K - \sigma_J'}\,d\sigma_J', \tag{10}$$

where $\sigma_K = x_K + iy_K \in \partial R_K$, and dashed quantities are integration variables on ∂R_J. The model does not allow vorticity creation so that the total vorticity enclosed by ∂R_K is invariant. Hence from (8) and (9) the area $A_K(t)$ of R_K varies as

$$A_K(t) = A_K(0)\exp[-\Omega(t)] \tag{11}$$

The initial value problem discussed before may be transformed into a two-dimensional flow.[11] Thus applying the similarity transformation,[7]

$$T = \int_0^t \exp[\Omega(t')]dt', \tag{12a}$$

$$\lambda(T) = \exp[\Omega(t(T))/2]\,\sigma(t(T)), \tag{12b}$$

to (10) gives

$$\frac{\partial \xi_K}{\partial T} - i\frac{\partial \eta_K}{\partial T} = -b(T)\exp[-\Omega(t(T))](\xi_K + i\eta_K) + \frac{\omega_0}{2\pi i}\sum_{J=1}^{M}\oint_{\partial R_J}\frac{\eta_K - \eta_J'}{\lambda_K - \lambda_J'}\,d\lambda_J', \tag{13}$$

where $\lambda = \xi + i\eta$ and $b(T) = \beta(t(T)) - \frac{1}{2}\gamma(t(T))$. This is a strictly two-dimensional vortex motion in a λ plane with time variable T, subject to a plane two-dimensional strain field with principal axes of strain along the ξ and η axes. The physics of the flow are unchanged; for the same initial conditions, the vortex boundary at T in the $\lambda(T)$ flow has the same shape as the corresponding boundary at time t in the $\sigma(t)$ flow but is altered in scale by a factor $\exp[\Omega(t)/2]$. Thus, as an alternative to (10), we could use (13) and deduce the effect of stretching from (12). No computational advantage results, however, and consequently the calculations reported here were done using (10).

III. NUMERICAL TREATMENT

For the present applications we take $\gamma = \gamma_0$ and $\beta = \beta_0$ as constants. Time and length scales are nondimensionalized against ω_0^{-1} and $[A(0)]^{1/2}$, respectively. Thus γ_0 and β_0 are dimensionless ratios of the strain rate constants to the initial vorticity. Since the CD technique is now well established, we give only a brief description of the algorithm used. We consider only a single vortex [$M = 1$ in Eq. (10)]. The vortex contour is descretized by first defining it as a set of N nodes $\sigma_j, j = 0 \cdots N$, $\sigma_0 = \sigma_N$, connected by straight lines or polynomial curves. Note that the subscript on σ now refers to node number. For the calculation of the integral in (11), ∂R is considered instantaneously to take the form of a closed poly-

gon. The contribution of each straight line segment in (σ_{j-1}, σ_j) may then be integrated exactly to give the velocity, $\partial x_k/\partial t - i\partial y_k/\partial t$ of the kth node as a function of σ_j, $j = 0 \cdots N$. In practice, the exact element contribution was used only for $|\sigma_k - \sigma_j| \leqslant r_{\text{crit}}$, where $r_{\text{crit}} = 0.1[A(t)]^{1/2}$. When $|\sigma_k - \sigma_j| > r_{\text{crit}}$, appropriate asymptotic forms of the complex logarithms were used, resulting in a substantial saving of execution time.

To maintain accuracy when ∂R becomes highly distorted, a node insertion/removal scheme was operated. Nodes were added by linear interpolation in (σ_j, σ_{j+1}), where

$$|\sigma_{j+1} - \sigma_j| > S, \tag{14}$$

$$S = \max[\min\{\Delta_{\min}/2,\ S_{\max},\ 1/2|\mathscr{K}|\},\ 0.021], \tag{15}$$

$$\Delta_{\min} = \max[\Delta_c,\ 0.04] \tag{16}$$

$$S_{\max} = \min[P/40, 0.15]. \tag{17}$$

In (14), Δ_c is the distance of closest approach of the segment from any vortex contour other than ∂R ($\Delta_c = \infty$ for the single vortex case). $\mathscr{K}$ is the local curvature and P the contour perimeter. The real numbers in (14)–(17) are empirical quantities obtained by numerical experimentation. The curvature was estimated as

$$\mathscr{K}_j = \frac{\text{Im}\{\partial\sigma^*/\partial e\ \partial^2\sigma/\partial e^2\}_j}{|\partial\sigma/\partial e|_j^3}, \tag{18}$$

where Im refers to the imaginary part and e is a contour parameter which was identified with local node number. Following node insertion, node σ_{j+1} was deleted where $|\sigma_{j+1} - \sigma_j| < 0.01, j = 0 \cdots N-1$, and the node set was renumbered. The $2N(t)$ ODE's were integrated forward in t using a standard fourth-order Runge–Kutta method. The time step Δt and time interval Δt_N between node insertion/removal were given by

$$\Delta t = c_1 \exp(-\gamma_0 t), \tag{19}$$

$$\Delta t_N = 3\Delta t,$$

where $c_1 \sim O(10^{-1})$ is a constant whose value depends on the application.

Several methods of checking the accuracy of the calculations were employed. First, the algorithm was tested against exact solutions[12] for isolated elliptical vortices (see Sect. IV A). This test is not comprehensive since these flows exhibit neither thin vortex filaments nor separate but arbitrarily close vortex boundaries. Second, a global error control was maintained by observing the time variation of the fractional error in the calculated contour area given by

$$E(t) = [\exp(\gamma_0 t)A(t) - A(0)]/A(0), \tag{20}$$

where $A(t) = 0.5\ \text{Im}[\int_{\partial R} \sigma^*\, d\sigma]$ is the calculated contour–polygon area. For an exact solution, (11) shows $E(t) \equiv 0$. Unfortunately (20) is rather insensitive to errors in position and shape of thin vortex filaments. It would therefore be desirable to follow the variation of other invariants of the motion as further means of error control. The total energy is an obvious choice but is rather difficult to calculate to the necessary accuracy and, moreover, requires renormalization because of the infinite contributions from the strain field and the generally nonvanishing total circulation. Third, for selected examples of the vortex coalescence calculations, the constants in (14)–(17) which control the node insertion/removal, scheme, and Δt in (19), were systematically varied in order to verify convergence of the contour shape as a function of time with increasing N. Specific examples are described subsequently.

IV. RESULTS AND DISCUSSION

A. Isolated elliptical vortices

Solutions for this flow have been obtained by Neu[12] who has shown that, for all γ_0 and β_0 (corresponding to $\gamma - \gamma'$ and $-\gamma'$, respectively, in his notation), an initial elliptical-shaped vortex remains elliptical, thus generalizing the classical rotating, nondeforming Kirchhoff vortex solution which holds for $\gamma_0 = \beta_0 = 0$. Three examples have been chosen for comparison with Neu's solutions by selecting initial conditions which correspond to oscillation, rotation, and infinite planar elongation of the ellipse for $\gamma_0 = 0$, $\beta_0 \neq 0$. The initial aspect ratio and orientation of the ellipse are specified by selecting a point on the phase-plane plot[12] in the region corresponding to the appropriate behavior. The strain rate γ_0 is then set to a nonzero value, and the time evolution of the ellipse calculated by the contour-dynamics algorithm. Figures 1(a)–1(c) show time sequences of these test cases, respectively. They are compared with the solutions of Neu obtained presently by integrating numerically his three coupled differential equations describing the evolution of the ellipse semimajor and semiminor axes and the angle of the semimajor axis to the x axis. The two sets of solutions show excellent agreement, both illustrating clearly

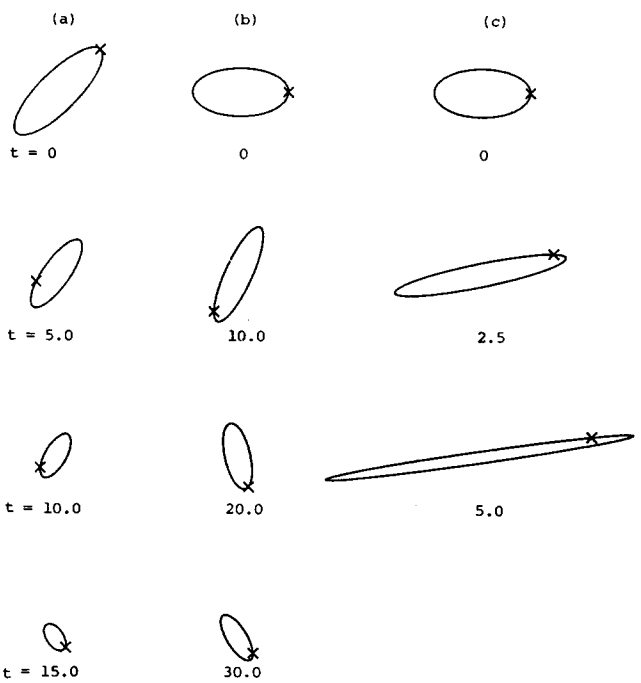

FIG. 1. Evolution of uniform vortices in a three-dimensional strain field. The × marks a material particle, and the times are shown on each drawing. The contour-dynamics solution is plotted as a solid line with the solution due to Neu[12] superimposed as a dashed line. These are indistinguishable on the scale shown. (a) $\gamma_0 = 0.15$, $\beta_0 = -0.12$, (b) $\gamma_0 = 0.05$, $\beta_0 = 0.084$, (c) $\gamma_0 = 0.015$, $\beta_0 = -0.25$.

the exponential area reduction according to (11). In the CD calculation $N = 30$ initially, and no node insertion or removal occurred over the calculated times. For the final frame of each sequence of Fig. 1, $E \sim O(10^{-3})$.

B. Coalescence of stretched vortices

For simplicity we restrict attention to plane three-dimensional stretching in the y-z plane with $\beta_0 = 0$, $\gamma_0 > 0$. Figures 2–5 show the effect of this strain field on the coalescence of two initially circular uniform vortices of equal strength. In Figs. 2–4, the plane of the vortex axes at $t = 0$ is normal to the y-z plane, while in Fig. 5 it lies in the y-z plane. The initial dimensionless vortex diameter is $d = (4/\pi)^{1/2}$, and values of the center separation $D = 1.50$, 1.70, and 1.92 were chosen to approximately match those used by Zabusky *et al.*[2] in their original computation of the $\gamma_0 = \beta_0 = 0$ case. Note that the vortex pair geometry, with $M = 2$ in Eq. (10), is constrained to give invariance under coordinate rotations of $n\pi$, $n = 1,2,\ldots$. Thus the motion of only one vortex is calculated explicitly. Results are shown as time sequences of vortex evolution for $\beta_0 = 0$ and $\gamma_0 = 0$, 0.05, 0.10, and 0.15. Each calculation was terminated either when $N \sim 0$ (500) (800 for Fig. 5) or when Δt became unacceptably small. In the final frame of each sequence $E \sim O(10^{-3})$.

Two principal effects of stretching are apparent from the $D = 1.50$ sequences of Fig. 2. First there is a slight increase in the speed of angular rotation of the merged structure with increasing γ_0 caused by vorticity intensification. Second, vortex stretching is seen to substantially inhibit the formation of spiral sheets of vorticity. At low or zero γ_0, these sheets are ejected from the main vortex core presumably to satisfy angular momentum and other conservation laws. They subsequently remain stable to local Kelvin–Helmholtz instability because of the stablizing effect of the two-dimensional (x–y) strain induced by the merged central vortex (see Moore[13] for an analysis of the stability of spiral vortex sheets). For the highest stretching rate ($\gamma_0 = 0.15$), the two vortices coalesce into an elongated "perturbed elliptical" shape with much attenuated embryo-spiral arms con-

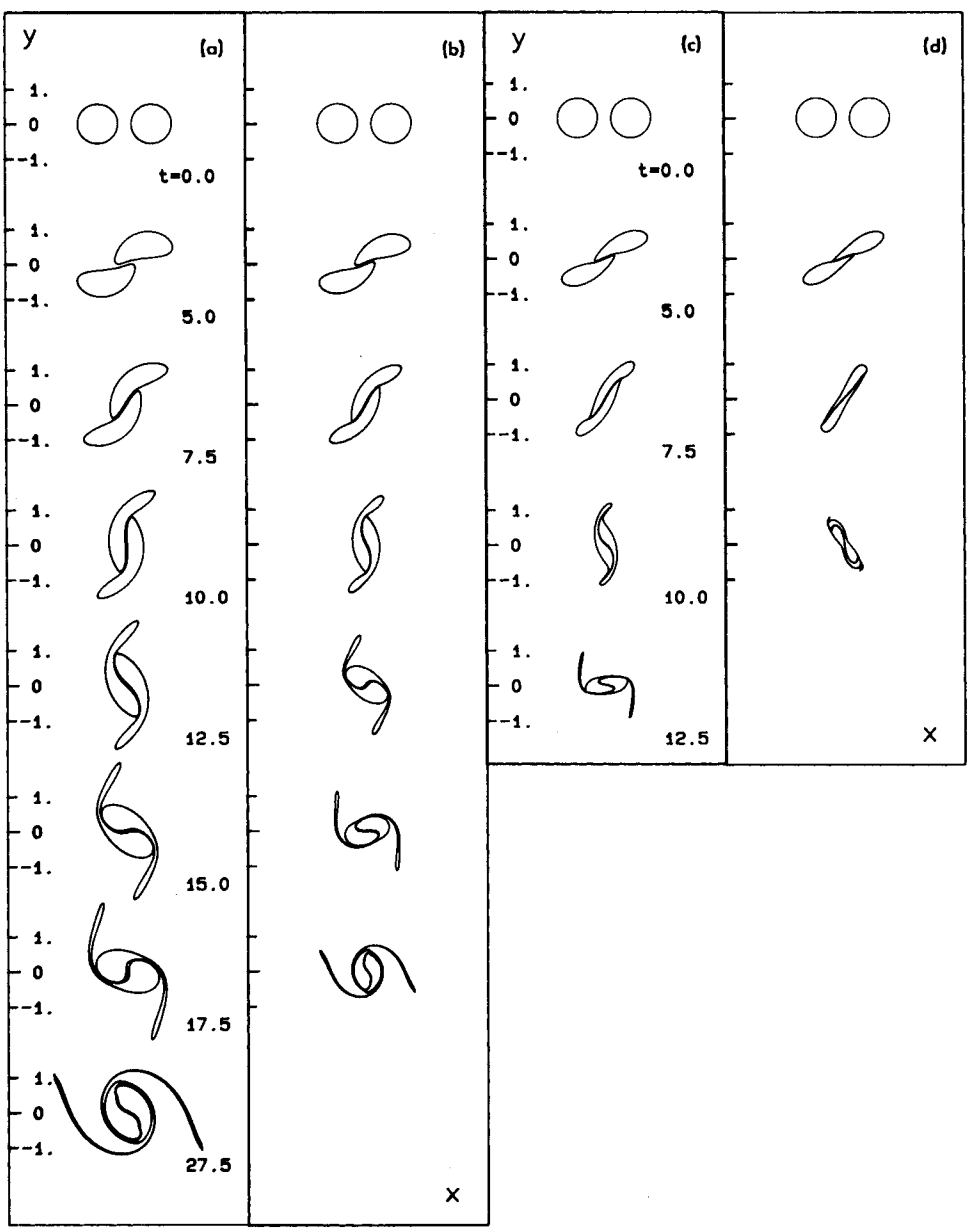

FIG. 2. Coalescence of equal uniform vortices in a stretching strain field with $\beta_0 = 0$. (a) $\gamma_0 = 0$, (b) $\gamma_0 = 0.05$, (c) $\gamma_0 = 0.10$, (d) $\gamma_0 = 0.15$. Times t as shown, $d = (4/\pi)^{1/2}$, $D = 1.50$ for (a)–(d).

taining little circulation. In fact, each of the vortex-sheets shown for $\gamma_0 = 0.10$ and 0.15 is actually a double sheet, one from each primary vortex. The formation of the inner sheet (nearer the vortex center) appears to be connected with apparent cusp formation in the vortex contour, for example in Fig. 2(c), $\gamma_0 = 0.1$ at $t = 7.5$. At $t = 12.5$ for $\gamma_0 = 0.1$, the inner sheet is of negligible thickness and the same is true for both sheets at $t = 10.0$ for $\gamma_0 = 0.15$ in Fig. 2(d).

For the related (but more unstable) problem of periodic vortex sheet motion, there is strong numerical[14] and asymptotic[15] evidence which indicates locally nonanalytic behavior of the sheet evolution, leading to the spontaneous formation of a curvature singularity in a finite time. The numerical calculation of the vortex sheet motion past the singularity in these cases remains a delicate and as yet unresolved matter.[16] The appearance of cusps on the vortex boundary here and in previous CD calculations[2–4] suggests possibly analogous behavior in the evolution of a vorticity discontinuity. The vanishingly thin vortex filaments which form from cusps may thus be entirely spurious, since the CD algorithm is quite unable to detect any singular behavior of the vortex boundary. Where these filaments are vanishingly thin and, therefore, have negligible global dynamic effect on the vortex motion, their suppression either by explicit smoothing or by the introduction of model terms in the CD equations[17] would seem to be justified. We note however that in Lundgren's[7] strained spiral-vortex model of turbulence fine structure at high Reynolds number, the mere existence of nonaxisymmetric vortex sheets leads to the $-5/3$ law for the turbulence energy spectrum.

To check the effect of increasing N on the shape of the vortex contour, the flows of Figs. 2(b) and 2(d) were repeated with the constants in (14)–(17) altered to give different numbers of nodes in the final stages of each calculation. At

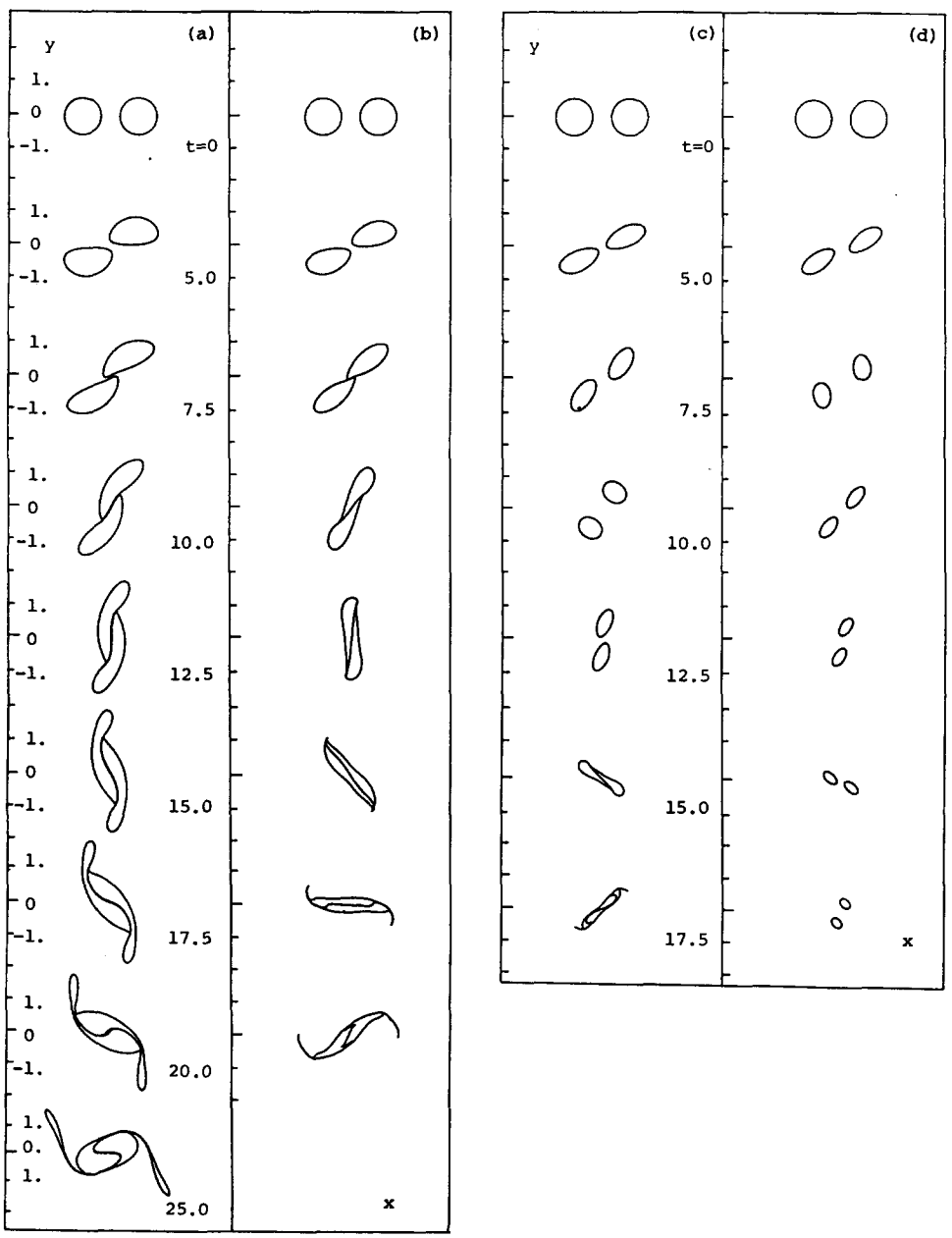

FIG. 3. Coalescence of equal uniform vortices in a stretching strain field with $\beta_0 = 0$. (a) $\gamma_0 = 0$, (b) $\gamma_0 = 0.05$, (c) $\gamma_0 = 0.10$, (d) $\gamma_0 = 0.15$. Times t as shown, $d = (4/\pi)^{1/2}$, $D = 1.70$ for (a)–(d).

$t = 17.5$ in Fig. 2(b), each vortex has $N = 435$. For a calculation of the same case with $N = 324$ at $t = 17.5$, the vortex contour was indistinguishable to within plotting accuracy from those shown in Fig. 2(b) at the same times. With $N = 160$ at $t = 17.5$, the final vortex contour was unchanged except for some small-scale irregularities near the vortex center. In three separate computations of the case shown in Fig. 2(d), the vortex contour at $t = 10.0$ was the same (to within plotting accuracy) with $N = 87$, 139, and 227, respectively. With $\gamma = 0$, 0.05, and 0.1 in Figs. 3(a)–3(c) with $D = 1.70$, the vortex merging process is qualitatively similar to that shown for $D = 1.50$, with the difference that for larger initial separation, spiral vortex-sheet formation is suppressed at lower values of γ_0. Increasing γ_0 further to $\gamma_0 = 0.15$ in Fig. 3(d) inhibits vortex coalescence altogether for $t < 17.5$. Continuation of this case past $t = 25.0$ (not displayed) showed no later-time tendency towards merging. Increasing the separation to $D = 1.92$ in Figs. 4(a)–(d) gives only weak merging interaction for $\gamma_0 = 0$. Coalescence is completely inhibited for $\gamma_0 > 0.05$, with each uniform vortex stretching ultimately to a line vortex while moving in an inwardly directed spiral trajectory. These tendencies agree qualitatively with those found by Lin and Corcos[9] in their numerical simulation of vortex coalescence in the late time evolution of the Burgers' strained vortex layer. Their calculations begin from the (perturbed) equilibrium Burgers' vortex sheet, and consequently, the Reynolds number (Re) is inversely proportional to $\gamma_0^{1/2}$. In two calculations at $\mathrm{Re} \sim O(10)$, Lin and Corcos obtain strong coalescence for the smaller value of γ_0 but no tendency toward merging for the larger value. This agreement may be fortuitous however, since in their configuration, there is an extra component of strain effectively present [absent in our calculations, but equivalent to finite $\beta_0 \sim O(\gamma_0)$] because of the doubly infinite vortex array.

The tendency toward strain-induced suppression of vortex merging seen in the present simulations, and possibly also in those of Ref. 9, may be understood qualitatively by considering the two-dimensional $\lambda(T)$ flow equivalent to each sequence in Figs. 2–4. From (13) these have $b(T) = -\frac{1}{2}\gamma_0$. Since $\gamma_0 > 0$, the vortex centers in Figs. 2–4 lie on the extensional principal (ξ) axis of strain at $T = 0$ for the $\lambda(T)$ flow. Hence the strain field tends to increase $D/A(0)^{1/2}$ for small T, thus inhibiting coalescence. This interpretation immediately suggests that positioning the vortex centers initially on the y axis (compressional principal axis of

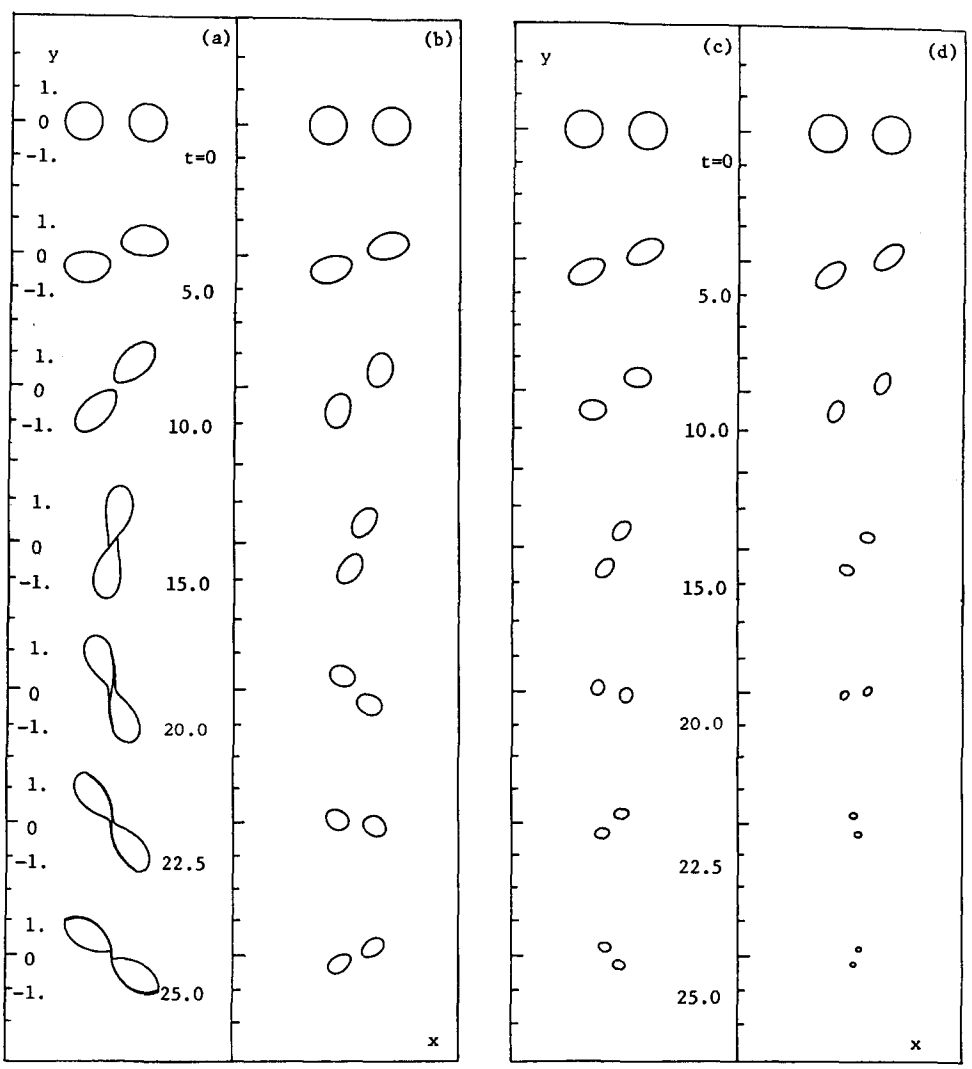

FIG. 4. Coalescence of equal uniform vortices in a stretching strain field with $\beta_0 = 0$. (a) $\gamma_0 = 0$, (b) $\gamma_0 = 0.05$, (c) $\gamma_0 = 0.10$, (d) $\gamma_0 = 0.15$. Times t as shown, $d = (4/\pi)^{1/2}$, $D = 1.92$ for (a)–(d).

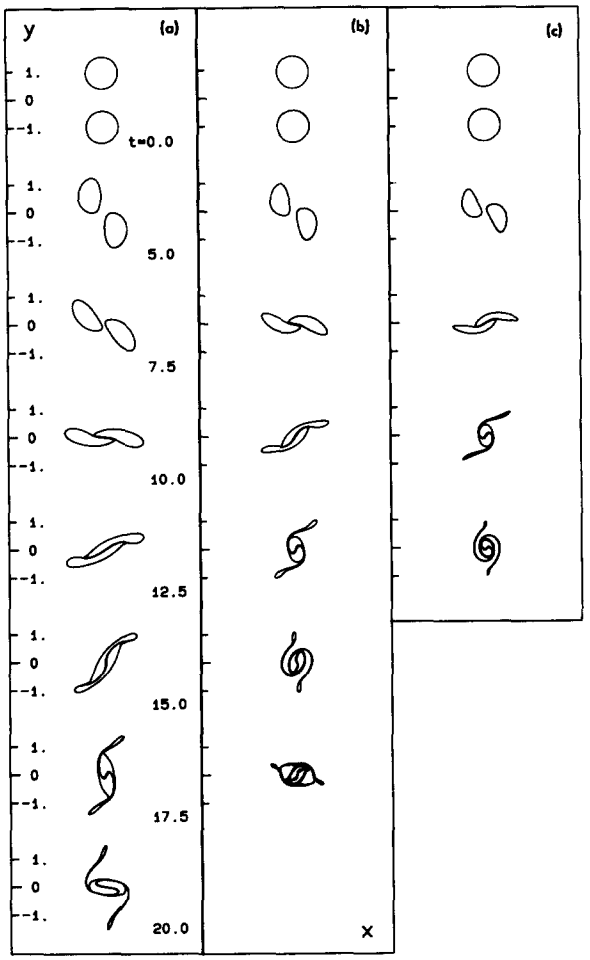

FIG. 5. Coalescence of equal uniform vortices in a stretching strain field with $\beta_0 = 0$. (a) $\gamma_0 = 0.05$, (b) $\gamma_0 = 0.10$, (c) $\gamma_0 = 0.15$. Times t as shown, $d = (4/\pi)^{1/2}$, $D = 1.92$ for (a)–(c).

strain for both the $\sigma(t)$ and $\lambda(T)$ flows with $\gamma_0 > 0$) would alter the qualitative effect of stretching. This is clearly demonstrated in Figs. 5(a)–5(c) where $D = 1.92$ and $\gamma_0 = 0.05$, 0.1, 0.15. Comparing these sequences with the equivalent unstrained flow in Fig. 4(a) shows that stretching now enhances coalescence, leading to well-developed spiral-sheet structure.

V. CONCLUSIONS

The present model of uniform inviscid vortex evolution in the presence of a stretching strain field was found to give good results in test comparisons with the analytical solutions of Neu[12] for the deformational behavior of isolated elliptical vortices. In the two-vortex interaction, plane three-dimensional strain in the y-z plane was found to significantly influence the detailed local geometry of the evolving vorticity distribution. The specific effect of stretching appears to depend on the initial relative orientation between the plane containing the vortex axes and the plane of the straining motion. When these planes are normal, the stretching strain field acts in order to increase the separation of the vortices relative to the cross-sectional vortex scale, thus inhibiting the formation of structural features associated with coalescence. This behavior is quite different from the effect of pure axially symmetric strain, which according to (10) and (13), merely rescales in length and time the unstrained ($\gamma_0 = \beta_0 = 0$) vortex-pair evolution.

The present simulations may be expected to be relevant to vortex coalescence in a real viscous fluid at sufficiently high Reynolds number over some finite time period prior to the onset of an approximate equilibrium between intensification of vorticity by the stretching strain field and its diffusion by viscosity. For pure axially symmetric stretching strain, the time scale for the decay of the spiral-merged vortex towards the axially symmetric Burgers'[10] solution is of order[7] (in dimensional coordinates) $t_\nu \omega_0 \sim \omega_0/\gamma_0 \log[1 + \mathrm{Re}\,\gamma_0/\omega_0]$, where Re = total circulation/ν. Individual spiral turns, once formed, decay on a rather shorter time scale. In the case of plane three-dimensional strain (and general nonsymmetric strain), the final state of the merged vortex may be a nonsymmetric Burgers' vortex of the type described by Robinson and Saffman,[18] with the corresponding decay time of order t_ν given above. The asymptotic state of cases where there is no merging remains uncertain.

ACKNOWLEDGMENT

This work was supported by the Australian Research Grants Scheme under Grant No. F 8315031 I.

[1] A. Leonard, J. Comput. Phys. **37**, 289 (1980).
[2] N. J. Zabusky, M. H. Hughes, and K. V. Roberts, J. Comput. Phys. **30**, 96 (1979).
[3] E. A. Overman, II and N. J. Zabusky, Phys. Fluids, **25**, 1297 (1982)
[4] D. I. Pullin, J. Fluid Mech. **108**, 401 (1981).
[5] P. G. Saffman and J. C. Schatzman, SIAM J. Sci. Stat. Comput. **2**, 285 (1981).
[6] A. E. Perry and M. S. Chong, J. Fluid Mech **119**, 173 (1982).
[7] T. S. Lundgren, Phys. Fluids **25**, 2193 (1982).
[8] G. M. Corcos and F. S. Sherman, J. Fluid Mech. **139**, 29 (1984).
[9] S. J. Lin and G. M. Corcos, J. Fluid Mech. **141**, 139 (1984).
[10] J. M. Burgers, in *Advances in Applied Mechanics* (Academic, New York, 1948), Vol. I, p. 198.
[11] T. S. Lundgren (private communication).
[12] J. Neu, Phys. Fluids **27**, 2397 (1984).
[13] D. W. Moore, Mathematica **23**, 35 (1976).
[14] D. I. Merion, G. R. Baker, and S. A. Orszag, J. Fluid Mech. **114**, 283 (1982).
[15] D. W. Moore, Proc. R. Soc. Lond. Ser. A **365**, 105 (1979).
[16] R. Krasny, submitted to J. Fluid Mech.
[17] N. J. Zabusky and E. A. Overman, II J. Comput. Phys. **52**, 351 (1983).
[18] A. C. Robinson and P. G. Saffman, Stud. Appl. Math., 163, (1984).